

## Comparison of acute phase response in mice after inhalation and intratracheal instillation of molybdenum disulphide and tungsten particles

Gutierrez, Claudia Torero; Loizides, Charis; Hafez, Iosif; Biskos, George; Loeschner, Katrin; Brostrøm, Anders; Roursgaard, Martin; Saber, Anne Thoustrup; Møller, Peter; More Authors

**DOI**

[10.1111/bcpt.13915](https://doi.org/10.1111/bcpt.13915)

**Publication date**

2023

**Document Version**

Final published version

**Published in**

Basic and Clinical Pharmacology and Toxicology

**Citation (APA)**

Gutierrez, C. T., Loizides, C., Hafez, I., Biskos, G., Loeschner, K., Brostrøm, A., Roursgaard, M., Saber, A. T., Møller, P., & More Authors (2023). Comparison of acute phase response in mice after inhalation and intratracheal instillation of molybdenum disulphide and tungsten particles. *Basic and Clinical Pharmacology and Toxicology*, 133(3), 265-278. Article 13915. <https://doi.org/10.1111/bcpt.13915>

**Important note**

To cite this publication, please use the final published version (if applicable).  
Please check the document version above.


**Copyright**

Other than for strictly personal use, it is not permitted to download, forward or distribute the text or part of it, without the consent of the author(s) and/or copyright holder(s), unless the work is under an open content license such as Creative Commons.

**Takedown policy**

Please contact us and provide details if you believe this document breaches copyrights.  
We will remove access to the work immediately and investigate your claim.

# Comparison of acute phase response in mice after inhalation and intratracheal instillation of molybdenum disulphide and tungsten particles

Claudia Torero Gutierrez<sup>1,2</sup> | Charis Loizides<sup>3</sup> | Iosif Hafez<sup>3</sup> |  
George Biskos<sup>3,4</sup> | Katrin Loeschner<sup>5</sup> | Anders Brostrøm<sup>2</sup> |  
Martin Roursgaard<sup>1</sup> | Anne Thoustrup Saber<sup>2</sup> | Peter Møller<sup>1</sup> |  
Jorid Birkelund Sørli<sup>2</sup> | Niels Hadrup<sup>2,6</sup> | Ulla Vogel<sup>2</sup> 

<sup>1</sup>Section of Environmental Health, Department of Public Health, University of Copenhagen, Copenhagen, Denmark

<sup>2</sup>National Research Centre for the Working Environment, Copenhagen, Denmark

<sup>3</sup>Climate and Atmosphere Research Centre, The Cyprus Institute, Nicosia, Cyprus

<sup>4</sup>Faculty of Civil Engineering and Geosciences, Delft University of Technology, Delft, The Netherlands

<sup>5</sup>Research Group for Analytical Food Chemistry, National Food Institute, Technical University of Denmark, Kongens Lyngby, Denmark

<sup>6</sup>Research Group for Risk-Benefit, National Food Institute, Technical University of Denmark, Kongens Lyngby, Denmark

## Correspondence

Ulla Vogel, National Research Centre for the Working Environment, Copenhagen, Denmark.

Email: [ubv@nfa.dk](mailto:ubv@nfa.dk)

## Funding information

This work was supported by the Focused Research Effort on Chemicals in the Working Environment (FFIKA) from the Danish Government and the Danish Working Environment Research Fund (grant No. 29-2019-09, "Sikker-Motor").

## Abstract

Inhalation studies are the gold standard for assessing the toxicity of airborne materials. They require considerable time, special equipment, and large amounts of test material. Intratracheal instillation is considered a screening and hazard assessment tool as it is simple, quick, allows control of the applied dose, and requires less test material. The particle-induced pulmonary inflammation and acute phase response in mice caused by intratracheal instillation or inhalation of molybdenum disulphide or tungsten particles were compared. End points included neutrophil numbers in bronchoalveolar lavage fluid, *Saa3* mRNA levels in lung tissue and *Saa1* mRNA levels in liver tissue, and SAA3 plasma protein. Acute phase response was used as a biomarker for the risk of cardiovascular disease. Intratracheal instillation of molybdenum disulphide or tungsten particles did not produce pulmonary inflammation, while molybdenum disulphide particles induced pulmonary acute phase response with both exposure methods and systemic acute phase response after intratracheal instillation. Inhalation and intratracheal instillation showed similar dose-response relationships for pulmonary and systemic acute phase response when molybdenum disulphide was expressed as dosed surface area. Both exposure methods showed similar responses for molybdenum disulphide and tungsten, suggesting that intratracheal instillation can be used for screening particle-induced acute phase response and thereby particle-induced cardiovascular disease.

## KEYWORDS

acute phase response, inhalation, intratracheal instillation, molybdenum disulphide, tungsten

This is an open access article under the terms of the [Creative Commons Attribution-NonCommercial](https://creativecommons.org/licenses/by-nc/4.0/) License, which permits use, distribution and reproduction in any medium, provided the original work is properly cited and is not used for commercial purposes.

© 2023 The Authors. *Basic & Clinical Pharmacology & Toxicology* published by John Wiley & Sons Ltd on behalf of Nordic Association for the Publication of BCPT (former Nordic Pharmacological Society).

## 1 | INTRODUCTION

Inhalation studies are considered the gold standard for evaluating the toxicity of airborne materials.<sup>1–3</sup> Inhalation studies are especially useful for regulatory purposes, as the Organization for Economic Co-operation and Development (OECD) made available guidelines for inhalation toxicity studies of nanomaterials. However, inhalation studies are expensive and require time, special equipment, and a large amount of test materials.<sup>2,4</sup> On the other hand, intratracheal (i.t.) instillation is considered a tool for screening and hazard assessment of airborne particles, as it allows control of the dose deposited in the lungs.<sup>5</sup> In addition, i.t. instillation is simple, faster, less expensive and does not require large quantities of material.<sup>2,6,7</sup>

Particle-induced acute phase response has been proposed as a new mechanism of action linking particle exposure to the risk of cardiovascular disease.<sup>8,9</sup> The mechanism of action has regulatory relevance, since a new suggestion for a health-based occupational exposure limit for zinc oxide was based on this mechanism of action.<sup>10</sup>

Acute phase response (APR) is the systemic reaction to inflammatory agents or conditions, for example, infectious agents, tissue injury, or advanced cancer. During APR, the concentration of acute phase proteins in the blood changes, for example, Serum Amyloid A (SAA) can increase as much as 1000 times in concentration.<sup>11</sup> APR is a well-established risk factor for cardiovascular disease.<sup>8,12–14</sup> We have previously suggested that particle inhalation and the development of cardiovascular disease are causally connected through APR.<sup>8,9,15</sup> In addition, we have previously shown that particle-induced pulmonary APR results in dose-dependent differential expression of several acute phase genes,<sup>8,9</sup> accompanied by dose-dependent increases in protein levels of several acute phase proteins.<sup>16,17</sup> We use *Saa3* as a biomarker of a pulmonary APR to particle exposure as the most differentially expressed gene. Thus, we have previously reported increased pulmonary inflammation, *Saa3* mRNA levels in lung tissue, *Saa1* mRNA in liver tissue, and SAA1/2 and SAA3 plasma levels in mice, after i.t. instillation of several nanomaterials including TiO<sub>2</sub>, carbon black, nanoclays, graphene, and multiwalled carbon nanotubes (MWCNT).<sup>16,18–24</sup> In addition, after repeated i.t. instillations of SAA in *ApoE*<sup>−/−</sup> mice, SAA3 plasma levels were elevated and accompanied by progression of aortic plaque formation.<sup>25</sup>

Molybdenum disulphide (MoS<sub>2</sub>) and tungsten (W) are used as spray-formulated lubricants for engines and were recently studied in inhalation studies to assess their effects on pulmonary inflammation and genotoxicity,<sup>26,27</sup>

but not their effect on APR. In the present study, we evaluate the effect MoS<sub>2</sub> and W have on pulmonary inflammation and APR after i.t. instillation and compare it to the results from the inhalation studies.

## 2 | MATERIALS AND METHODS

### 2.1 | Materials

MoS<sub>2</sub> powder (particle size <2 μm and purity of 98%) was purchased from Sigma-Aldrich (Cat. No. 234842), while W powder (particle size <1 μm and purity of 99.95%) was obtained from Alfa Aesar (Cat. No. 44210). Carbon black (Printex 90) was a kind gift from Degussa-Hüls (today Evonic, Germany) and was used as a benchmark material for pulmonary inflammation and APR.<sup>5,18,22,28–34</sup>

The surface area of both materials was measured using nitrogen absorption Brunauer, Emmett, and Teller (BET) analysis (3P sync 110) as described in the literature.<sup>26,27</sup> In brief, samples were dried at 200°C under vacuum for 2 h, weighed, and then analysed using the static volumetric technique method with nitrogen as the adsorbate. The results showed that MoS<sub>2</sub> had a specific surface area of 8.96 m<sup>2</sup>/g and W of 1.38 m<sup>2</sup>/g.<sup>26,27</sup>

### 2.2 | Suspension and characterization

A pilot study was first carried out to determine the dose levels used in this study. For both materials, one mouse was i.t. instilled with 162 μg and observed for 1 day for symptoms of discomfort or marked weight loss. If the dose was tolerated, it was selected as the high dose level. In our tests, 162 μg/mouse was selected as the high dose level and 54 μg/mouse as the low dose level, for both materials.

The particles were dispersed in 2% v/v C57BL/6 mouse serum in Nanopure water to prepare the high dose level, which was then sonicated on ice for 16 min at 10% amplitude using a Branson Sonifier S-450D (Branson Ultrasonics Corp., USA). Additionally, the vehicle solution (Nanopure water with 2% mouse serum) was sonicated without any particles for exposure control. The suspensions were three times diluted in vehicle solution and then sonicated for four additional minutes to achieve the low dose level.

A Malvern Zetasizer Nano ZS (Malvern Instruments, UK), Dynamic Light Scattering (DLS) was used to determine the hydrodynamic size distribution and polydispersity index of the particles in suspension. For each dose level, six readings from the exposure suspension were recorded ( $n = 1$ ).

Primary particle size and particle size distribution were measured by scanning electron microscopy analysis. In order to generate samples, a total of four suspensions were made by dispersing the W and MoS<sub>2</sub> powders in ethanol, which was dropcast onto transmission electron microscopy (TEM) grids. The two W solutions had concentrations of 1.1 and 3.3 mg/ml, while the two MoS<sub>2</sub> solutions had concentrations of 1.1 and 3.4 mg/ml. These concentrations were chosen to resemble those that were used for i.t. instillation. Each suspension was sonicated for 10 min prior to adding 10 µl of the given suspension directly onto Formvar/Carbon-coated Ni TEM grids with mesh 400. The grids were left under a glass lid for 2 min before excess liquid was blotted away with a tissue. The four samples were analysed with an Apreo 2 C LoVac SEM (Thermo-Fisher Scientific—FEI) at an acceleration voltage of 10 keV and a beam current of 0.4 nA. The images were acquired in immersion mode, using the T2 in-lens detector. Most images were acquired at a magnification of 5k with an image size of 6144 × 4376 pixels, resulting in a resolution of 6.74 nm/pixel. Some higher resolution images were also acquired of individual particles for display purposes. For size distribution measurements, the images were analysed with the Amira-Avizo 2D Analyser software (Thermo-Fisher Scientific—FEI). Here, a Gaussian filter was initially applied for denoising, followed by a hysteresis threshold to distinguish particles from the substrate. Further data handling and plotting were made with Python. Primary particle sizes were obtained by manually fitting an ellipse onto 30 individual particles using the ImageJ/Fiji software.<sup>35</sup> All particle sizes are reported as equivalent circular diameters.

## 2.3 | Animal housing

The present study was carried out over a period of 24 days. Five- and six-week-old female C57BL/6J mice (Janvier Labs, France) were randomly placed in polypropylene cages and allowed to acclimatize for 2 to 3 weeks. Mice exposed to the vehicle control were housed in groups of three and, in the case of particle exposure, in groups of six. Enrichment materials included wood blocks, nesting material and shelters (Brogaarden, Denmark), and Enviro-dri bedding. Mice had unlimited access to food (Altromin 1324 M, Brogaarden, Denmark) and water and were exposed to 12-h light and dark cycles. The temperature was set at 20 ± 2°C and the humidity at 50 ± 20%. The study was conducted in accordance with the Basic & Clinical Pharmacology & Toxicology policy for experimental and clinical studies.<sup>36</sup>

## 2.4 | Intratracheal instillation

The intratracheal instillations were performed on three different calendar days according to the material that was going to be instilled (MoS<sub>2</sub>, W, or Printex 90), and mice were euthanized the following days (i.e., 24 h post-exposure). Specifically, the intratracheal instillations and ensuing euthanasia were performed over 9 days. The protocol used for the intratracheal instillation has been published in Jackson et al.<sup>37</sup> In brief, the mice were first anaesthetized by inhalation of isoflurane at 4% concentration. Then, 50 µl of vehicle control or particle suspension was i.t. instilled, followed by 150 µl of air. Based on previous studies, we used group sizes of  $n = 3$  mice as vehicle control on every exposure day and  $n = 6$  mice for each dose level of material; this group size allows the detection of relevant differences for pulmonary inflammation. For W and MoS<sub>2</sub>, mice were instilled with 54 µg/mouse (1.08 mg/ml) as low dose level and 162 µg/mouse (3.24 mg/ml) as high dose level; 162 µg/mouse (3.24 mg/ml) was used for Printex 90. The mice were monitored to make sure their airways were not obstructed after instillation.

## 2.5 | Inhalation studies

The inhalation studies were performed nose-only with mice placed in tubes that were inserted into the inhalation chamber and have been previously reported in Sørli et al.<sup>26,27</sup> In the MoS<sub>2</sub> inhalation study, male BALB/c mice ( $n = 8$  for all exposure groups) were exposed for 30 min/day, 5 days/week for 3 weeks in the case of MoS<sub>2</sub>. Three dose levels were used (i.e., low dose, mid dose, and high dose) with air MoS<sub>2</sub> concentrations of 3, 50, and 150 mg/m<sup>3</sup>. The study observed the mid and high exposure level groups had a lower weight gain than the control groups. Additionally, a decrease in respiratory tidal volume was observed in the mice groups exposed to the low and high doses on day 15 of exposure. Pulmonary inflammation was obtained in the high dose group only; while increased genotoxicity was observed in BAL fluid cells from groups exposed to mid and high exposure levels.<sup>26</sup>

In the case of the W study, male BALB/c mice ( $n = 8$  for all exposure groups) were exposed for 45 min/day, 5 days/week for 2 weeks, and three dose levels were used with air concentrations of 9, 23, and 132 mg/m<sup>3</sup>. No changes in body weight were observed in any of the exposure groups. Although there was no pulmonary inflammation, genotoxicity was observed in BAL fluid cells from the low and high exposure groups, suggesting primary genotoxicity. Finally, a decrease in plasma testosterone was found in mice from the low exposure group.<sup>27</sup>

## 2.6 | Blood, BAL fluid, and tissue collection

One day after intratracheal instillation, mice were anaesthetised with a ZRF cocktail (Zoletil Forte 250 mg/ml, Rompun 20 mg/ml, and Fentanyl 50 µg/ml in sterile isotonic saline) by intraperitoneal injection, using a dose of 0.1 ml per 10-g body weight. After ensuring that the mice were under anaesthesia, by checking position and withdrawal reflexes, they were euthanized by exsanguination. Heart blood was collected with a syringe, mixed with 0.17-M K<sub>2</sub>EDTA, and kept on ice.<sup>37</sup> The blood samples were centrifuged for 10 min at 2500 g and 4°C to obtain plasma.

The lungs were flushed twice with 0.8 ml of 0.9% sodium chloride, and the bronchoalveolar lavage (BAL) fluid was collected and kept on ice.<sup>32</sup> The BAL fluid samples were centrifuged at 400 g and 4°C for 10 min. Ham's F-12 medium containing 10% foetal bovine serum was used to resuspend the cell pellet. Mouse lung and liver tissue were collected, cut into sections, snap frozen in liquid nitrogen, and then stored at -80°C.

## 2.7 | Cell differential counting

Using a Cytofuge 2 cytocentrifuge (VWR—Bie and Berntsen, Denmark) for 4 min at 60 g, cells collected from BAL fluid were concentrated onto microscope slides. After centrifugation, slides were air-dried for 30 min and then fixed for 5 min in 96% ethanol. After that, cells were stained for 30 min with Giemsa stain and for 3 min with May–Grünwald stain. Samples were randomized and blinded. Light microscopy was used to count and categorize 200 cells per sample in order to perform a differential count.

## 2.8 | *Saa3* and *Saa1* gene expression

Gene expression was performed on lung and liver tissues collected in the present study and on tissues collected during the inhalation studies using MoS<sub>2</sub> and W.<sup>26,27</sup> *Saa3* mRNA levels were quantified in lung samples, and *Saa1* mRNA levels were quantified in liver samples as described by Poulsen et al. Using the Maxwell<sup>®</sup> 16 LEV simplyRNA tissue kit (Cat. No. AS1280, Promega) and according to the manufacturer's instructions, RNA was extracted from frozen tissue. A Nanodrop 200c spectrophotometer (Thermo-Fisher Scientific, USA) was used to quantify RNA concentrations. Then, complementary DNA was synthesized using TaqMan<sup>™</sup> Reverse Transcriptase reagents (Cat. No. N8080234, Thermo-Fisher Scientific). A modified TaqMan<sup>™</sup> Fast Advance Master Mix procedure was used

to determine the expression of both genes (Cat. No. 4444557, Thermo-Fisher Scientific). The *Saa3* analysis in lung tissue was performed using a forward primer (140909J1C12:5'-GCC TGG GCT GCT AAA GTC AT-3'), a reverse primer (40909J1B05: 5'-TGC TCC ATG TCC CGT GAA C-3'), and a *Saa3* probe (6-FAMTCT GAA CAG CCT CTC TGG CAT CGCT -TAMRA) from TAG Copenhagen. The *Saa1* analysis in liver tissue was performed using a primer/probe mix (Mm00656927\_g1) from Thermo-Fisher Scientific. The samples were analysed in triplicates using the ViiA 7 Real-time PCR system (Thermo-Fisher Scientific) and 18S gene as reference (Cat. No. 4310893E, Thermo-Fisher Scientific).<sup>18,38</sup>

## 2.9 | SAA3 plasma protein level

SAA3 protein levels were measured in plasma from mice exposed to the vehicle control, and the high dose level of MoS<sub>2</sub> and Printex 90, from the present i.t. instillation study as previously described.<sup>18</sup> In addition, we measured SAA3 from the medium and high dose level groups from the inhalation study of MoS<sub>2</sub>.<sup>26</sup> SAA3 plasma levels were quantified using a mouse SAA3 ELISA kit (Cat. No. EZMSAA3-12K, Merck Millipore). Samples were measured in duplicates according to the manufacturer's instructions.

## 2.10 | Alveolar deposition and retained lung burden

The alveolar deposition for MoS<sub>2</sub> and W were estimated in the inhalation studies by Sørli et al.<sup>26,27</sup>; the Multiple-Path Particle Dosimetry Model (MPPD) was used for the respective air exposure levels and exposure time. Retained lung burden of MoS<sub>2</sub> was measured in the inhalation study by Sørli et al.<sup>26</sup> In short, right lungs from exposed mice were weighed and digested with 67–69% nitric acid in a microwave reaction system. After digestion, samples were diluted with ultrapure water and 2% nitric acid, prior to analysis. The total mass concentration of Mo was determined by inductively coupled plasma mass spectrometry (ICP-MS), and deposited MoS<sub>2</sub> was calculated assuming a lung weight of 175 mg. Retained lung burden of W was not measured since the estimated deposition was low.<sup>27</sup>

## 2.11 | Statistics

GraphPad Prism 9 (GraphPad Software Inc., USA) was used to analyse all data, and results are presented as mean ± standard deviation. All outcome data were

logarithmically transformed using the base of 10 for the statistical analysis. The inhalation and i.t. instillation studies were designed independently and present intrinsic differences; therefore, within each exposure method, we have used one-way ANOVA and a post-hoc Dunnett's comparison test to compare the results from the vehicle control group to the exposure groups. Results from the control groups from the two inhalation studies were combined and data from the control groups for the instillation studies were combined, but data from instillation and inhalation controls were not combined. Linear regression analysis was used to assess differences in dose–response relationships (i.e., slopes) between i.t. instillation and inhalation exposures. Slopes and *r*-values correspond to relationships with logarithmically transformed outcomes and predictors in either normal scale (i.e., doses) or logarithmic scale (i.e., number of neutrophils or SAA3).

### 3 | RESULTS

#### 3.1 | Alveolar deposition and retained lung burden

The estimated deposition of MoS<sub>2</sub> and W have been previously reported in Sørli et al.<sup>26,27</sup> For MoS<sub>2</sub>, an alveolar deposition of 7, 27, and 79 μg MoS<sub>2</sub>/mouse was estimated based on the MPPD model, corresponding to the low, medium, and high exposure levels; while for W, a deposition of 1, 2, and 13 μg W/mouse was estimated. The retained lung burden from the MoS<sub>2</sub> inhalation study has been previously reported in Sørli et al.<sup>26</sup> The low, medium, and high exposure levels from the inhalation study resulted in a retained lung burden of 35, 101, and 171 μg MoS<sub>2</sub>/mouse, respectively.

#### 3.2 | Hydrodynamic particle size

The hydrodynamic size distribution in exposure suspensions was measured using DLS. The number-based size distribution (Figure 1) showed that both materials had unimodal peaks, at 106 nm for MoS<sub>2</sub> and 122 nm for W, while the Z-average size for MoS<sub>2</sub> was 461 nm and 439 nm for W, both measured at 3.24 mg/ml (162 μg/mouse). The polydispersity index was 0.39 for MoS<sub>2</sub> and 0.36 for W.

#### 3.3 | Primary particle size and particle size distribution

Representative secondary electron images from W and MoS<sub>2</sub> samples are shown in Figure 2 (top and bottom

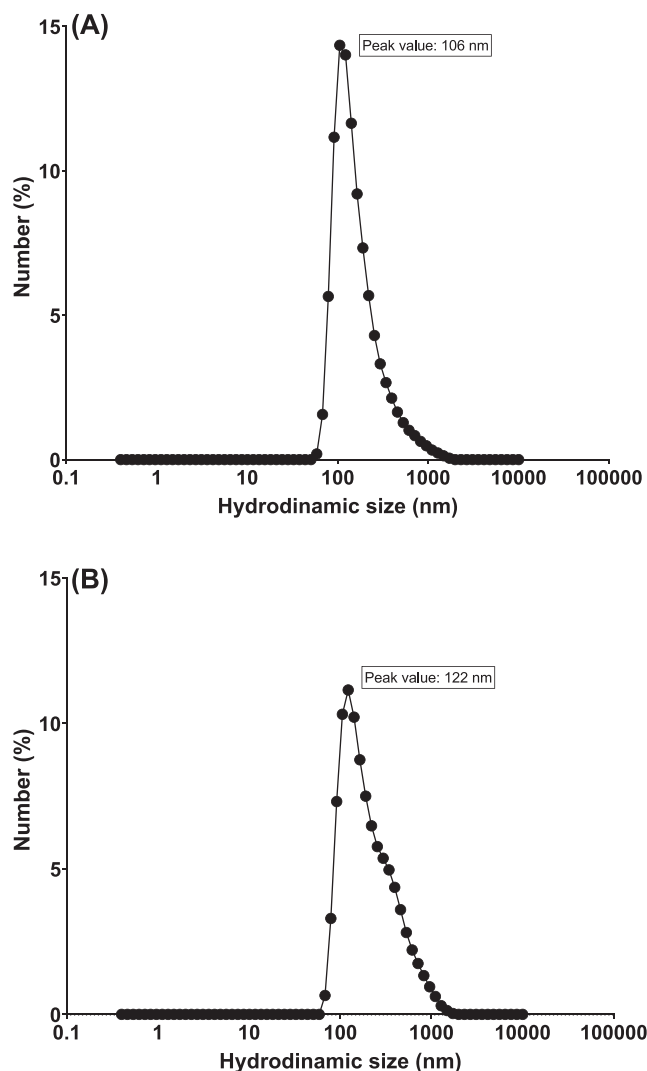


**FIGURE 1** Number-based hydrodynamic size distributions of (A) MoS<sub>2</sub> and (B) W, dispersed in instillation vehicle measured by dynamic light scattering. Both materials were measured using a concentration of at 3.24 mg/ml (162 μg/mouse).

rows, respectively). From the top row images, it is clear that the W particles primarily formed agglomerates in the micro size range. The agglomerates were dense and compact, but some were forked with chains of primary particles protruding in one or more directions. The agglomerates typically contained tens of primary particles that varied significantly in size. The primary particle size analysis, conducted on 30 individual particles, found an average size of  $160 \pm 147$  nm. Here, the largest measured size was 508 nm, while the smallest was 23 nm. This highlights the significant size variation of the primary particles, which covered more than an order of magnitude. The equivalent circular diameter distributions (Figure 3) show the agglomerate size peak at approximately 0.8 μm for 1 mg/ml W which is significantly smaller than for the 3 mg/ml sample, where the peak was

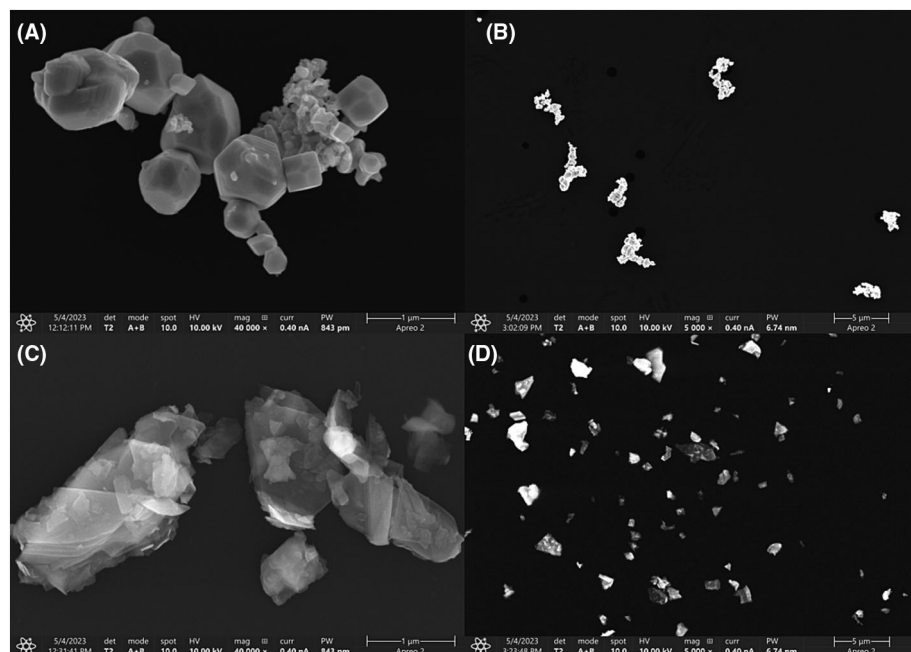


**FIGURE 2** Representative images from W (A and B) and MoS<sub>2</sub> samples (C and D). High-resolution images showing the morphology of a typical particle are presented in (A) and (C); while typical images used for size distribution measurements are shown in (B) and (D).

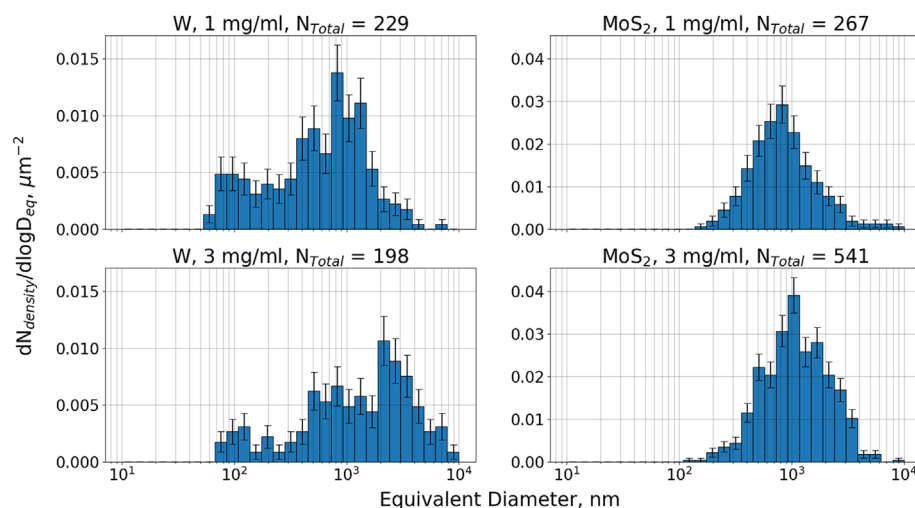


**FIGURE 3** Equivalent circular diameter distributions by number density from W (left column) and MoS<sub>2</sub> (right column) samples. Error bars were determined based on counting statistics as the square root of the number count. The total number of analysed particles from each sample are shown in the plot titles.

observed at approximately 2  $\mu\text{m}$ . This indicates that the increased concentration enhanced the level of agglomeration of the primary particles, resulting in larger sizes. However, the overall shape and number densities of the two size distributions appeared similar, with a tail extending down to approximately 100 nm, while the number density dropped to zero at 10  $\mu\text{m}$ .

The MoS<sub>2</sub> particles appeared very different from the W particles. The MoS<sub>2</sub> particles were observed as flakes or sheets. In some cases, the flakes overlapped, but in general, they were more often observed as single flakes rather than agglomerates as opposed to the W sample. Based on measurements of 30 individual flakes, the primary particle size analysis gave an average primary size of  $392 \pm 212$  nm. Here, the largest measured flake was

1  $\mu\text{m}$ , while the smallest was 97 nm, again displaying a broad range of primary particle sizes spanning an order of magnitude. It should be noted that the primary particle analysis of the MoS<sub>2</sub> flakes is highly uncertain due to the challenge of distinguishing thin overlapping flakes in agglomerates and due to the less rounded particle shape, which resulted in poor fittings of the elliptical shape. From the MoS<sub>2</sub> equivalent circular diameter distributions in the right column of Figure 3, it is observed that both samples show a single peak starting at approximately 200 nm and ending at 3–4  $\mu\text{m}$ . The peak was shifted slightly to 1  $\mu\text{m}$  for the 3 mg/ml sample compared with approximately 800 nm for the 1 mg/ml sample. This indicates that the level of agglomeration was either similar for the two samples or that the flaky nature of the MoS<sub>2</sub>

particles makes them agglomerate differently, for example, layering sheets rather than joining at the edges. The number densities were also comparable for the two samples, though slightly higher for the 3 mg/ml sample.

### 3.4 | BAL fluid cell composition

Pulmonary inflammation was assessed as the number of neutrophils in the BAL fluid. Neutrophil numbers from the inhalation studies have been previously reported in Sørli et al.<sup>26,27</sup> The results showed that i.t. instillation of MoS<sub>2</sub> or W did not produce an elevation of neutrophil numbers, which was only significantly induced by our benchmark material (Printex 90) (Figure 4). This suggests that i.t. instillation of neither MoS<sub>2</sub> nor W induced pulmonary inflammation by the dose levels used. The total BAL fluid cell composition can be found in Supporting Information S1.

### 3.5 | *Saa3* and *Saa1* mRNA levels

We used mRNA levels of *Saa3* in lung tissue and *Saa1* in liver tissue as biomarkers of the pulmonary and hepatic APR, respectively.<sup>9</sup> Our results (Figure 5) show a dose-dependent increase in *Saa3* mRNA levels in lung tissue from mice exposed to MoS<sub>2</sub> by inhalation, while in the case of i.t. instillation, only the high dose of MoS<sub>2</sub> and Printex 90 induced a statistically significant increase of *Saa3* mRNA levels in lungs. In the case of liver *Saa1* mRNA levels, neither inhalation of MoS<sub>2</sub> nor W produced a significant elevation of mRNA levels. I.t. instillation of these materials did not produce an increase of *Saa1* mRNA levels in liver tissue, with the

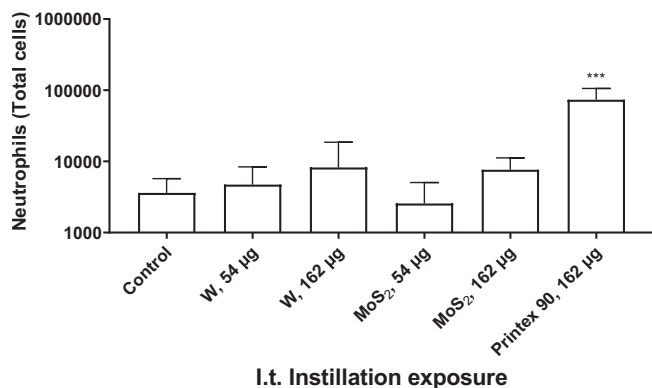


**FIGURE 4** Neutrophil numbers in BAL (bronchoalveolar lavage) fluid 1 day after i.t. instillation of W, MoS<sub>2</sub>, or carbon black (Printex 90). Data are shown as mean and bars represent SD. \*\*\* designates *p*-values < 0.001 versus control.

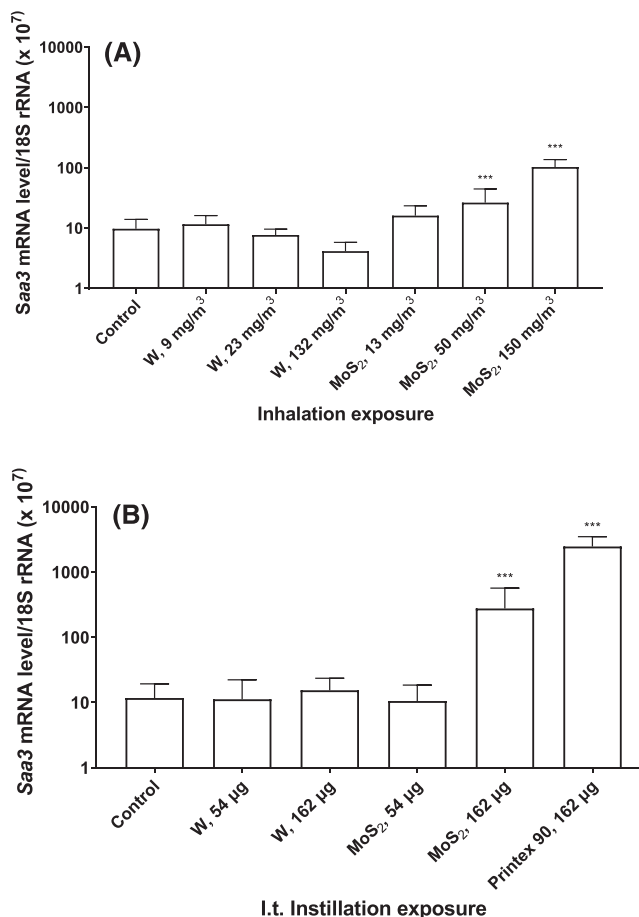


**FIGURE 5** *Saa3* mRNA levels in lung tissue after inhalation (A) or i.t. instillation (B) of W, MoS<sub>2</sub>, or carbon black (Printex 90). Data are shown as mean and bars represent SD. \*\*\* designates *p*-values < 0.001 versus control.

exception of the low dose of MoS<sub>2</sub> (Figure 6). We did not see any elevation of *Saa3* nor *Saa1* mRNA levels in mice exposed to W, by inhalation nor instillation. The results suggest that MoS<sub>2</sub> exposure induced pulmonary APR, while W exposure did not at the assessed dose levels.

### 3.6 | SAA3 protein plasma levels

We measured SAA3 protein levels in plasma from mice exposed to MoS<sub>2</sub>, both by inhalation and i.t. instillation exposures. We did not include samples from exposure to W, as none of the exposure methods elevated *Saa3* mRNA levels in the lungs. From both studies, we selected the dose levels that increased *Saa3* mRNA levels. Our results (Figure 7) showed that only the i.t. instillation of the high dose of MoS<sub>2</sub> and Printex 90 increased the plasma levels of SAA3. This finding suggests that high pulmonary *Saa3* expression is accompanied by a systemic APR.



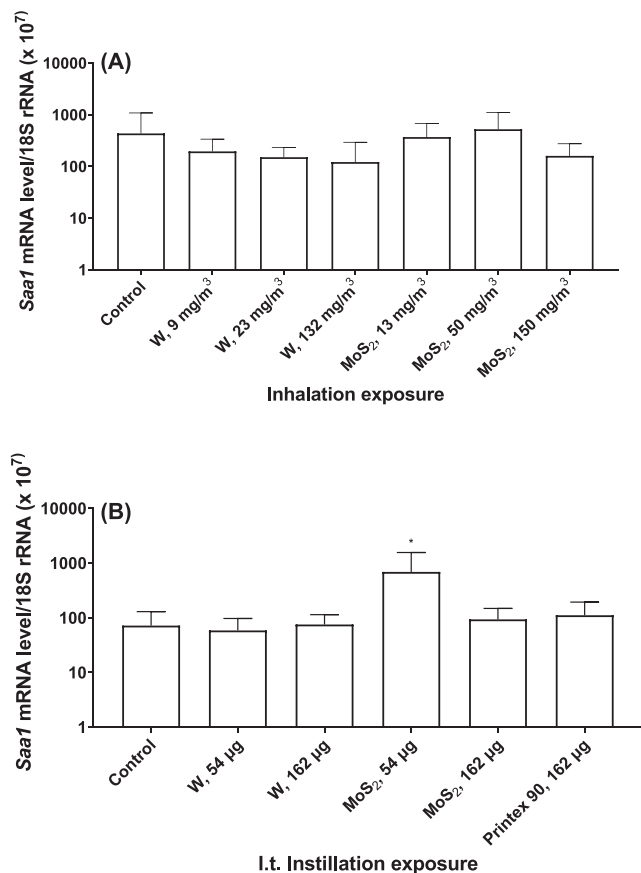


**FIGURE 6** *Saa1* mRNA levels in liver tissue after inhalation (A) or i.t. instillation (B) of W, MoS<sub>2</sub>, or carbon black (Printex 90). Data are shown as mean and bars represent SD. \* designates *p*-values < 0.05 versus control.

### 3.7 | Comparison between exposure methods for MoS<sub>2</sub>

Figure 8 presents the neutrophil numbers, *Saa3* mRNA level in lung tissue, and SAA3 plasma protein as function of the deposited dose levels of MoS<sub>2</sub> expressed as surface area (i.e., deposited surface area) for both exposure methods. Sørli et al.<sup>26</sup> reported that the specific surface area of MoS<sub>2</sub> was 8.96 m<sup>2</sup>/g, and the retained lung burden of MoS<sub>2</sub> (measured as Mo) was estimated to be 35, 101, and 171 µg MoS<sub>2</sub>/mouse, respectively, for low, medium, and high exposure levels. In the case of the i.t. instillation study, we assumed the instilled dose was fully deposited in the lungs, that is, 54 and 162 µg MoS<sub>2</sub>/mouse, respectively, for low and high exposure levels. We used the retained surface area as it correlates to pulmonary inflammation and APR.<sup>8,9,39,40</sup> MoS<sub>2</sub> induced more pulmonary inflammation when dosed by inhalation (slope: 0.08; 95% CI: 0.06 to 0.10) than i.t. instillation (slope: 0.03; 95% CI: -0.003 to 0.06) (Figure 8A), while the *Saa3* mRNA levels showed similar dose-response

relationships for the two exposure methods (inhalation slope: 0.06; 95% CI: 0.05 to 0.07; instillation slope: 0.08; 95% CI: 0.05 to 0.12) (Figure 8B). In the case of SAA3 (Figure 8C), the dose-response relationships were also similar (inhalation slope: 0.005; 95% CI: -0.004 to 0.01; instillation slope: 0.02; 95% CI: 0.005 to 0.04).

We obtained significant correlations (see Supporting Information S1) between neutrophil numbers and *Saa3* mRNA levels (inhalation:  $R^2 = 60$ ; slope: 0.73; 95% CI: 0.57 to 0.89; instillation:  $R^2 = 0.79$ ; slope: 1.7; 95% CI: 1.4 to 1.99). In addition, we found significant correlations between neutrophil numbers and SAA3 plasma protein for i.t. instillation ( $R^2 = 0.85$ ; slope: 0.7; 95% CI: 0.54 to 0.86) and *Saa3* mRNA levels and SAA3 plasma protein levels for i.t. instillation ( $R^2 = 0.81$ ; slope: 0.41; 95% CI: 0.30 to 0.51).

## 4 | DISCUSSION

Inhalation studies are the gold standard for evaluating the toxicity of respirable materials. Usually, these studies assess the material-induced toxicity in rats in terms of pulmonary inflammation, histopathology, cardiovascular disease end points, genotoxicity, and cancer. As an alternative to inhalation, i.t. instillation is a simple, inexpensive, and very practical methodology for hazard identification.<sup>5,6</sup> Here, we propose that APR can be used as a quantitative biomarker of particle-induced cardiovascular disease. Mice and humans have similar APR, and both express the acute phase protein SAA. SAA is causally implicated in atherosclerosis.<sup>14,41</sup> Thus, inactivation of all inducible SAA isoforms in mice leads to decreased formation of atherosclerotic plaques in *ApoE*<sup>-/-</sup> mice, while overexpression or i.t. instillation of SAA leads to increased formation of atherosclerotic plaques.<sup>25,41,42</sup> Conversely, for rats, there is not a registered SAA gene identification number in National Centre for Biotechnology Information as rats do not express the protein and this species has a fundamentally different APR than mice and humans. Therefore, rats have been considered less suited as an animal model for particle-induced atherosclerosis than dyslipidaemic mice.

In the present study, we i.t. instilled MoS<sub>2</sub> and W in mice and assessed pulmonary inflammation and APR 1 day post-exposure and compared this with corresponding inhalation studies,<sup>26,27</sup> in order to evaluate the potential use of i.t. instillation for hazard assessment of particle-induced APR. Repeated inhalation studies (acute or subchronic inhalation studies) are the studies normally used for risk and hazard assessment of particles in order to be able to assess the possible toxicological effects of a cumulative lung burden. In addition, repeated

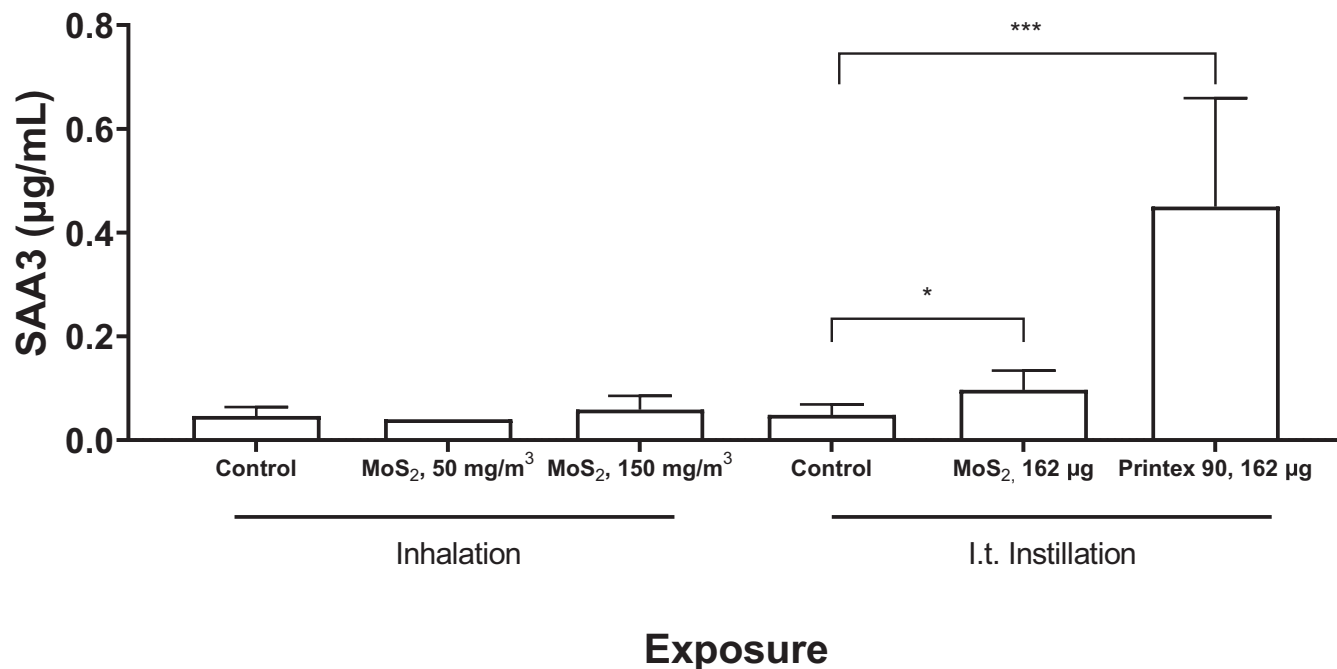


**FIGURE 7** SAA3 protein levels in plasma, after inhalation or i.t. instillation of MoS<sub>2</sub> or carbon black (Printex 90). Data are shown as mean and bars represent SD. \* and \*\*\* designate *p*-values < 0.05 and < 0.001, respectively, *versus* control.

exposures are often needed in inhalation studies to reach sufficient lung burden to induce particle-induced pulmonary inflammation. For example, in the study by Gaté et al., rats were exposed to a multiwalled carbon nanotube material (MWCNT) by inhalation (0.5 or 1.5 mg/m<sup>3</sup> for 2 × 3 h/day, 5 days/week for 4 weeks) or a single i.t. instillation (180 or 540 µg/rat). It was estimated that the lung burden obtained from the highest concentration used during inhalation was comparable with the lung burden from the lowest instilled dose.<sup>2</sup>

Neutrophil influx in BAL fluid was used as a biomarker of inflammation. We have previously shown that neutrophil influx is accompanied by strong inflammatory and APRs following inhalation of titanium dioxide nanoparticles, along with increased expression of genes related to inflammation and APR in mice.<sup>43,44</sup> Likewise, we have observed similar association after pulmonary exposure to several nanomaterials including carbon black, titanium dioxide, carbon nanotubes, graphene, and cobalt/iron metal oxides.<sup>9,16,17,28,45–55</sup> Particle-induced inflammation has also been demonstrated at protein level in lung tissue, where pulmonary exposure to carbon nanoparticles induced dose-dependent increases in protein levels of IL1b, IL3, IL6, IL12B, IL13, IL17, CCL2, CCL4, CXCL1, CXCL2, G-CSF, GM-CSF, IFN-γ, and TNF in lung tissue.<sup>56</sup> Moreover, we have previously observed that pulmonary inflammation in terms of neutrophil influx coincides with histopathological changes such as macrophages aggregates and lymphocytes infiltrates in lung

tissue after exposure to different carbon black nanomaterials.<sup>57</sup> Similarly, *Saa3* was used as a biomarker of APR. We have previously shown that increased *Saa3* expression is accompanied by dose-dependent increases in the number of differentially expressed acute phase response<sup>9</sup> as well as by increased blood levels of SAA3.<sup>18,23,26,58</sup> While i.t. instillation of MoS<sub>2</sub> and W did not cause pulmonary inflammation, MoS<sub>2</sub> induced pulmonary APR following both methods of exposure and systemic APR after i.t. instillation. Exposure to W did not cause pulmonary inflammation nor APR after i.t. instillation or inhalation.<sup>27</sup>

It is well-known that inflammation is predicted by the total surface area of the pulmonary deposited particles.<sup>39,40,59,60</sup> Recent studies have shown that APR is also correlated with pulmonary deposited surface area.<sup>8,9,22</sup> Both materials used in this study have high densities (5.06 for MoS<sub>2</sub> and 19.28 g/cm<sup>3</sup> for W), resulting in low specific surface areas of 8.96 and 1.38 m<sup>2</sup>/g, respectively, even though the particle size distribution and DLS showed the presence of nanosized particles. Therefore, a low total surface area was deposited following inhalation and i.t. instillation, which explains the low or lack of responses obtained for both materials, but more noticeable with W.

When assessing the dosed MoS<sub>2</sub> as surface area by both exposure methods, we obtained that the inhaled dose induced more inflammation than the i.t. instilled dose. Other studies have shown that i.t. instillation of

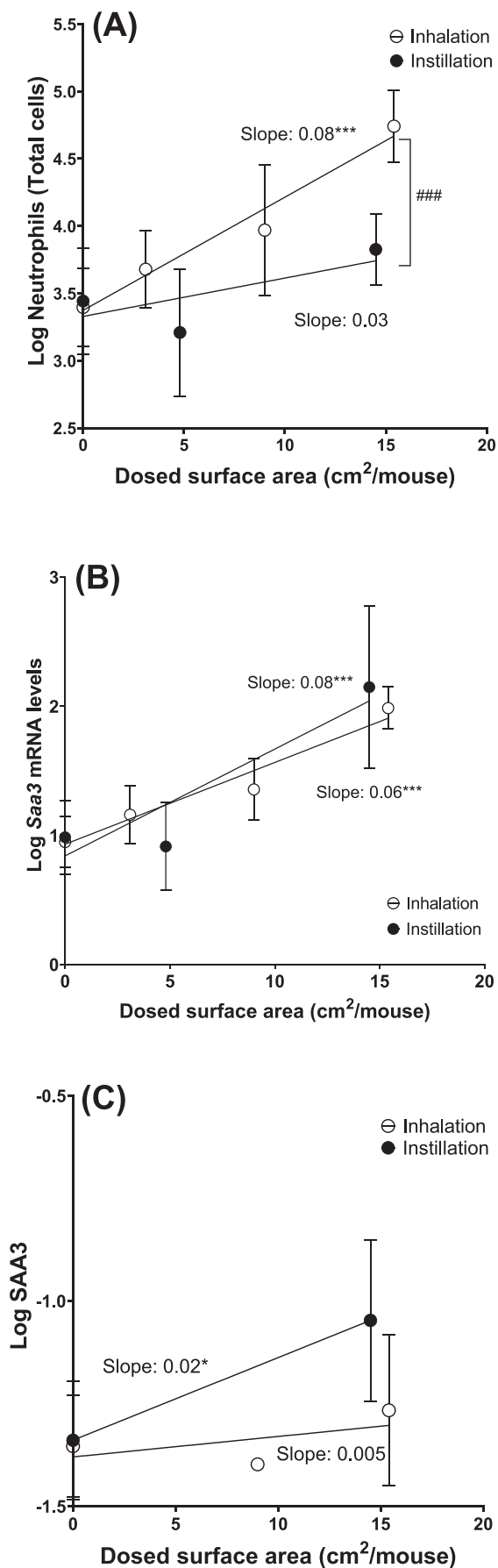


**FIGURE 8** Comparison of neutrophil number (A), *Saa3* mRNA level (B), and SAA3 protein level (C) between inhalation and i.t. instillation of MoS<sub>2</sub>. Dose is presented as deposited surface area. Points represent mean and bars represent SD. \* and \*\*\* designate *p*-values < 0.05 and < 0.001, respectively. ### represents a significant difference between slopes. Neutrophil data from the inhalation study are results from Sørli et al.<sup>26</sup>

nanomaterials produces similar or higher pulmonary inflammation than inhalation. Jackson et al. exposed female C57BL/6BomTac to Printex 90, by inhalation (1 h/day for 11 days) and four times i.t. instillations. They obtained a greater pulmonary inflammation after i.t. instillation than inhalation, even while using an estimated similar dose level.<sup>61</sup> Baisch et al. exposed F344 rats to TiO<sub>2</sub> using whole-body inhalation for 4 h and i.t. instillation. Even though they obtained similar lung burdens of TiO<sub>2</sub>, i.t. instillation exposure produced a higher number of neutrophils in BALF than inhalation when assessed after 24 h. In another study, Gaté et al. also compared the effect of exposing Sprague–Dawley rats using 4-week nose-only inhalation or single i.t. instillation of MWCNT. In that study, pulmonary inflammation was similar for inhalation and i.t. instillation exposure when the deposited dose was used as a predictor.

In the present study, the observed difference in the pulmonary neutrophil influx might be caused by differential pulmonary deposition of particles in the alveolar region of the lungs during the inhalation study as compared with i.t. instillation.<sup>62,63</sup> Nanosized particles have a high alveolar deposition during inhalation. As nanoparticles have a higher surface area to mass ratio than bigger particles,<sup>8,63</sup> the total deposited surface area during inhalation may be higher than the one deposited during i.t. instillation where particle deposition is not determined by particle aerosolization. Nonetheless, differential deposition of smaller particles might not be the only explanation for the difference between both exposure methods, as the pulmonary APR was similar when normalized to the total deposited surface area.

Another point to take into account when comparing results from inhalation and i.t. instillation is the difference in the mice used in each type of exposure. It has been shown that some strains are more sensitive to certain exposures than others. For example, C57BL/6 mice developed less pulmonary inflammation, in terms of neutrophil numbers in BAL fluid, than BALB/c mice, after being exposed to inflammatory substances such as ozone or cigarette smoke<sup>64,65</sup>; however, C57BL/6 mice are more prone to develop fibrosis after bleomycin administration than BALB/c mice.<sup>66</sup> In the case of gender, female mice

presented less inflammation than male mice, after oropharyngeal aspiration of lipopolysaccharide, in both C57BL/6 and BALB/c mice.<sup>67</sup> Therefore, the lower inflammatory response seen during i.t. instillation might be due to the use of female C57BL/6J in comparison with male BALB/cJ mice. Female C57BL/6J mice were used in the i.t. instillation study to enable comparison with previous i.t. instillation studies. Figure 9 shows that the present data align well with previous data on other insoluble metal-containing particles.

When comparing APR following inhalation and i.t. instillation of MoS<sub>2</sub>, the dose–response relationship for pulmonary *Saa3* expression and systemic SAA3 levels were similar, while neutrophil influx appeared much stronger following inhalation as compared with i.t. instillation exposure for MoS<sub>2</sub>. When looking at SAA3 plasma protein levels, we only had one significantly increased SAA3 response at one dose level from the i.t. instillation, although the data points fit to the same dose–response relationship.

We have previously shown that neutrophil numbers, *Saa3* mRNA levels, and SAA3 plasma protein levels are correlated to each other<sup>38</sup> when mice are i.t. instilled with metal oxide and Printex 90 nanomaterials. In this study, we obtained similar correlations between neutrophil numbers and *Saa3* mRNA levels, and between *Saa3* mRNA levels and SAA3 plasma protein levels. This finding provides additional evidence that these three end points can be used interchangeably as biomarkers of particle-induced APR, also when materials of larger particle size are tested. While data on neutrophil influx, *Saa3* mRNA levels, and SAA3 plasma levels are available from animal studies, only blood levels of acute phase proteins are available from human studies. In a previous study of metal oxide nanoparticle-induced APR in mice,<sup>38</sup> we compared the No Observed Adverse Effect Level (NOAEL) for zinc oxide (ZnO), when the NOAEL was derived based on induction of APR following i.t. instillation in mice and from a controlled human exposure study. The derived NOAELs appeared to be in the same order of magnitude. Furthermore, at the request of the Danish Working Environment Authority, the Danish National Research Centre for the Working Environment has prepared documentation for an occupational exposure limit for ZnO based on ZnO induction of APR as the critical effect.<sup>10</sup>

I.t. instillation is a fast, simple, and inexpensive method for toxicity testing of respirable materials, and it allows for control of the lung-deposited dose. Even though it does not mimic human exposure, we have previously shown, using i.t. instillation of Evans blue solution, radioactively labelled gold nanoparticles, quantum dots, and MWCNT, that i.t. instillation distributes

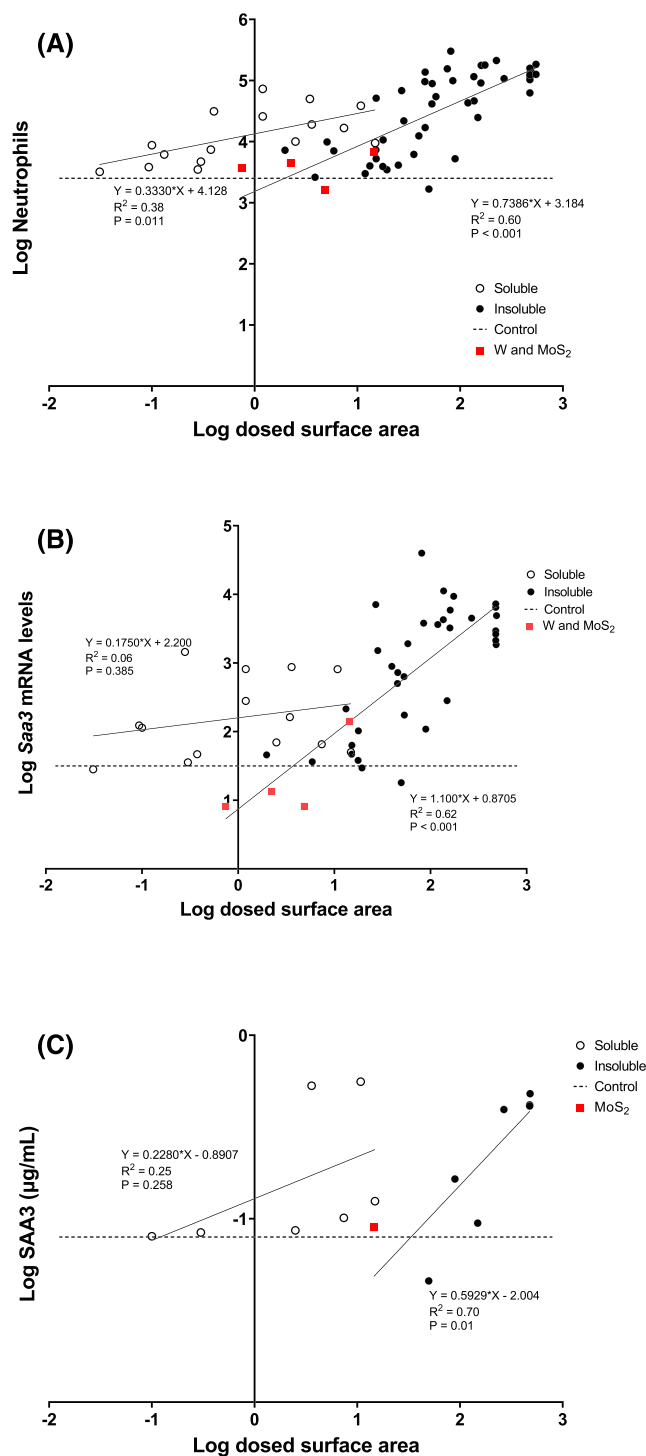


**FIGURE 9** Correlation analysis from the present study and previous studies assessing metal-containing particles, 1 day after i.t. instillation. The panes show (A) correlations between dosed surface area and neutrophil numbers, (B) dosed surface area and *Saa3* mRNA levels in lung tissue, and (C) dosed surface area and plasma SAA3. Results from the present study were combined with data from Gutierrez et al.<sup>38</sup>

particles into all lung lobes.<sup>30,68</sup> Our study has weaknesses due to differences in mice gender and strain between the two types of exposure. However, despite

these limitations, we have shown that the dose–response relationship between deposited surface area and pulmonary and systemic APR produced by inhalation and i.t. instillation is similar. This adds to the study by Gaté et al. mentioned previously, which found similar dose–response relationships between deposited surface area and neutrophil influx following inhalation and i.t. instillation exposure to MWCNT in rats. Therefore, the studies suggest that i.t. instillation can be used for hazard ranking and screening of APR produced by inhaled materials and thus for the screening in relation to assessment of risk of cardiovascular disease. Additionally, i.t. instillation can be used to prioritize materials for inhalation studies, leading to the optimization and reduction of the use of laboratory animals.

In summary, the present study shows that inhalation and instillation exposure exhibit similar responses for MoS<sub>2</sub> and W, suggesting that i.t. instillation can be used for screening particle-induced acute phase response and thereby particle-induced cardiovascular disease.

## ACKNOWLEDGEMENTS

The authors would like to thank Michael Gulbrandsen, Noor Irmam, Yasmin Akhtar, Anne Abildtrup, and Sarah Søs Poulsen for their expert technical assistance.

## CONFLICT OF INTEREST STATEMENT

The authors declare that they have no conflict of interests.

## DATA AVAILABILITY STATEMENT

The data used and/or during the current study are available from the corresponding author upon reasonable request.

## ORCID

Ulla Vogel  <https://orcid.org/0000-0001-6807-1524>

## REFERENCES

- Baisch BL, Corson NM, Wade-Mercer P, et al. Equivalent titanium dioxide nanoparticle deposition by intratracheal instillation and whole body inhalation: the effect of dose rate on acute respiratory tract inflammation. *Part Fibre Toxicol.* 2014; 11(1):1-16. doi:10.1186/1743-8977-11-5
- Gaté L, Knudsen KB, Seidel C, et al. Pulmonary toxicity of two different multi-walled carbon nanotubes in rat: comparison between intratracheal instillation and inhalation exposure. *Toxicol Appl Pharmacol.* 2019;375(May):17-31. doi:10.1016/j.taap.2019.05.001
- Morimoto Y, Izumi H, Yoshiura Y, et al. Comparison of pulmonary inflammatory responses following intratracheal instillation and inhalation of nanoparticles. *Nanotoxicology.* 2016; 10(5):607-618. doi:10.3109/17435390.2015.1104740
- Kinaret P, Ilves M, Fortino V, et al. Inhalation and oropharyngeal aspiration exposure to rod-like carbon nanotubes induce similar airway inflammation and biological responses in mouse lungs. *ACS Nano.* 2017;11(1):291-303. doi:10.1021/acsnano.6b05652
- Bendtsen KM, Gren L, Malmborg VB, et al. Particle characterization and toxicity in C57BL/6 mice following instillation of five different diesel exhaust particles designed to differ in physicochemical properties. *Part Fibre Toxicol.* 2020;17(1):1-25. doi:10.1186/s12989-020-00369-9
- Costa DL, Lehmann JR, Winsett D, Richards J, Ledbetter AD, Dreher KL. Comparative pulmonary toxicological assessment of oil combustion particles following inhalation or instillation exposure. *Toxicol Sci.* 2006;91(1):237-246. doi:10.1093/toxsci/kfj123
- Morimoto Y, Izumi H, Yoshiura Y, Fujishima K, Yatera K, Yamamoto K. Usefulness of intratracheal instillation studies for estimating nanoparticle-induced pulmonary toxicity. *Int J Mol Sci.* 2016;17(2):1-12. doi:10.3390/ijms17020165
- Hadrup N, Zhernovkov V, Jacobsen NR, et al. Acute phase response as a biological mechanism-of-action of (nano)particle-induced cardiovascular disease. *Small.* 2020;16(21):1907476. doi:10.1002/smll.201907476
- Saber AT, Jacobsen NR, Jackson P, et al. Particle-induced pulmonary acute phase response may be the causal link between particle inhalation and cardiovascular disease. *Wiley Interdiscip Rev Nanomed Nanobiotechnol.* 2014;6(6):517-531. doi:10.1002/wnan.1279
- National Research Centre for the Working Environment. Zinc oxide: scientific basis for setting a health-based occupational exposure limit. Published 2021. Accessed May 11, 2023. <https://nfa.dk/da/Forskning/Strategiske-forskningsomraader/Kemisk-arbejdsmiljo/Graensevaerdier>
- Gabay C, Kushner I. Acute-phase proteins and other systemic responses to inflammation. Epstein FH, ed. *N Engl J Med.* 1999;340(6):448-454. doi:10.1056/NEJM199902113400607
- Ridker PM, Hennekens CH, Buring JE, Rifai N. C-reactive protein and other markers of inflammation in the prediction of cardiovascular disease in women. *N Engl J Med.* 2000;342(12):836-843. doi:10.1056/NEJM200003233421202
- Zewinger S, Drechsler C, Kleber ME, et al. Serum amyloid A: high-density lipoproteins interaction and cardiovascular risk. *Eur Heart J.* 2015;36(43):3007-3016. doi:10.1093/eurheartj/ehv352
- Shridas P, Tannock LR. Role of serum amyloid A in atherosclerosis. *Curr Opin Lipidol.* 2019;30(4):320-325. doi:10.1097/MOL.0000000000000616
- Vogel U, Cassee FR. Editorial: dose-dependent ZnO particle-induced acute phase response in humans warrants re-evaluation of occupational exposure limits for metal oxides. *Part Fibre Toxicol.* 2018;15(1):5-7. doi:10.1186/s12989-018-0247-3
- Husain M, Saber AT, Guo C, et al. Pulmonary instillation of low doses of titanium dioxide nanoparticles in mice leads to particle retention and gene expression changes in the absence of inflammation. *Toxicol Appl Pharmacol.* 2013;269(3):250-262. doi:10.1016/j.taap.2013.03.018
- Jackson P, Hougaard KS, Vogel U, et al. Exposure of pregnant mice to carbon black by intratracheal instillation: toxicogenomic effects in dams and offspring. *Mutat Res - Genet Toxicol Environ Mutagen.* 2012;745(1-2):73-83. doi:10.1016/j.mrgentox.2011.09.018

18. Poulsen SS, Knudsen KB, Jackson P, et al. Multi-walled carbon nanotubephysicochemical properties predict the systemic acute phase response following pulmonary exposure in mice. *PLoS ONE*. 2017;12(4):1-26. doi:10.1371/journal.pone.0174167
19. Danielsen PH, Knudsen KB, Štrancar J, et al. Effects of physicochemical properties of TiO<sub>2</sub> nanomaterials for pulmonary inflammation, acute phase response and alveolar proteinosis in intratracheally exposed mice. *Toxicol Appl Pharmacol*. 2020; 386(October 2019):114830. doi:10.1016/j.taap.2019.114830
20. Di Ianni E, Møller P, Mortensen A, et al. Organomodified nanoclays induce less inflammation, acute phase response, and genotoxicity than pristine nanoclays in mice lungs. *Nanotoxicology*. 2020;14(7):869-892. doi:10.1080/17435390.2020.1771786
21. Saber A, Jacobsen N, Mortensen A, et al. Nanotitanium dioxide toxicity in mouse lung is reduced in sanding dust from paint. *Part Fibre Toxicol*. 2012;9(1):4. doi:10.1186/1743-8977-9-4
22. Saber AT, Lamson JS, Jacobsen NR, et al. Particle-induced pulmonary acute phase response correlates with neutrophil influx linking inhaled particles and cardiovascular risk. Morty RE, ed. *PLoS ONE*. 2013;8(7):e69020. doi:10.1371/journal.pone.0069020
23. Bengtson S, Knudsen KB, Kyjovska ZO, et al. Differences in inflammation and acute phase response but similar genotoxicity in mice following pulmonary exposure to graphene oxide and reduced graphene oxide. *PLoS ONE*. 2017;12(6):1-25. doi:10.1371/journal.pone.0178355
24. Poulsen SS, Saber AT, Mortensen A, et al. Changes in cholesterol homeostasis and acute phase response link pulmonary exposure to multi-walled carbon nanotubes to risk of cardiovascular disease. *Toxicol Appl Pharmacol*. 2015;283(3):210-222. doi:10.1016/j.taap.2015.01.011
25. Christophersen DV, Møller P, Thomsen MB, et al. Accelerated atherosclerosis caused by serum amyloid A response in lungs of ApoE<sup>-/-</sup> mice. *FASEB j*. 2021;35(3):1-14. doi:10.1096/fj.202002017R
26. Sørli JB, Jensen ACØØ, Mortensen A, et al. Pulmonary toxicity of molybdenum disulphide after inhalation in mice. *Toxicology*. 2023;485:153428. doi:10.1016/j.tox.2023.153428
27. Sørli JB, Jensen ACØ, Mortensen A, et al. Genotoxicity in the absence of inflammation after tungsten inhalation in mice. *Environ Toxicol Pharmacol*. 2023;98(January):104074. doi:10.1016/j.etap.2023.104074
28. Hadrup N, Rahmani F, Jacobsen NR, et al. Acute phase response and inflammation following pulmonary exposure to low doses of zinc oxide nanoparticles in mice. *Nanotoxicology*. 2019;13(9):1275-1292. doi:10.1080/17435390.2019.1654004
29. Hadrup N, Aimonen K, Ilves M, et al. Pulmonary toxicity of synthetic amorphous silica—effects of porosity and copper oxide doping. *Nanotoxicology*. 2021;15(1):96-113. doi:10.1080/17435390.2020.1842932
30. Poulsen SS, Jackson P, Kling K, et al. Multi-walled carbon nanotube physicochemical properties predict pulmonary inflammation and genotoxicity. *Nanotoxicology*. 2016;10(9):1263-1275. doi:10.1080/17435390.2016.1202351
31. Saber AT, Mortensen A, Szarek J, et al. Toxicity of pristine and paint-embedded TiO<sub>2</sub> nanomaterials. *Hum Exp Toxicol*. 2019; 38(1):11-24. doi:10.1177/0960327118774910
32. Kyjovska ZO, Jacobsen NR, Saber AT, et al. DNA damage following pulmonary exposure by instillation to low doses of carbon black (Printex 90) nanoparticles in mice. *Environ Mol Mutagen*. 2015;56(1):41-49. doi:10.1002/em.21888
33. Bendtsen KM, Brostrøm A, Koivisto AJ, et al. Airport emission particles: exposure characterization and toxicity following intratracheal instillation in mice. *Part Fibre Toxicol*. 2019;16(1):23. doi:10.1186/s12989-019-0305-5
34. Barfod KK, Bendtsen KM, Berthing T, et al. Increased surface area of halloysite nanotubes due to surface modification predicts lung inflammation and acute phase response after pulmonary exposure in mice. *Environ Toxicol Pharmacol*. 2020; 73(July 2019):103266. doi:10.1016/j.etap.2019.103266
35. Schneider CA, Rasband WS, Eliceiri KW. NIH image to ImageJ: 25 years of image analysis. *Nat Methods*. 2012;9(7):671-675. doi:10.1038/nmeth.2089
36. Tveden-Nyborg P, Bergmann TK, Jessen N, Simonsen U, Lykkesfeldt J. BCPT policy for experimental and clinical studies. *Basic Clin Pharmacol Toxicol*. 2021;128(1):4-8. doi:10.1111/bcpt.13492
37. Jackson P, Lund SP, Kristiansen G, et al. An experimental protocol for maternal pulmonary exposure in developmental toxicology. *Basic Clin Pharmacol Toxicol*. 2011;108(3):202-207. doi:10.1111/j.1742-7843.2010.00644.x
38. Gutierrez CT, Loizides C, Hafez I, et al. Acute phase response following pulmonary exposure to soluble and insoluble metal oxide nanomaterials in mice. *Part Fibre Toxicol*. 2023;20(1):4. doi:10.1186/s12989-023-00514-0
39. Oberdorster G, Ferin J, Lehnert BE. Correlation between particle size, in vivo particle persistence, and lung injury. *Environ Health Perspect*. 1994;102(SUPPL. 5):173-179. doi:10.1289/ehp.102-1567252
40. Cosnier F, Seidel C, Valentino S, et al. Retained particle surface area dose drives inflammation in rat lungs following acute, subacute, and subchronic inhalation of nanomaterials. *Part Fibre Toxicol*. 2021;18(1):1-21. doi:10.1186/s12989-021-00419-w
41. Thompson JC, Wilson PG, Shridas P, et al. Serum amyloid A3 is pro-atherogenic. *Atherosclerosis*. 2018;268(3):32-35. doi:10.1016/j.atherosclerosis.2017.11.011
42. Dong Z, Wu T, Qin W, et al. Serum amyloid A directly accelerates the progression of atherosclerosis in apolipoprotein E-deficient mice. *Mol Med*. 2011;17(11):1357-1364. doi:10.2119/molmed.2011.00186
43. Hougaard KS, Jackson P, Jensen KA, et al. Effects of prenatal exposure to surface-coated nanosized titanium dioxide (UV-titan). A study in mice. *Part Fibre Toxicol*. 2010;7(1):16. doi:10.1186/1743-8977-7-16
44. Halappanavar S, Jackson P, Williams A, et al. Pulmonary response to surface-coated nanotitanium dioxide particles includes induction of acute phase response genes, inflammatory cascades, and changes in microRNAs: a toxicogenomic study. *Environ Mol Mutagen*. 2011;52(6):425-439. doi:10.1002/em.20639
45. Billing AM, Knudsen KB, Chetwynd AJ, et al. Fast and robust proteome screening platform identifies neutrophil extracellular trap formation in the lung in response to cobalt ferrite nanoparticles. *ACS Nano*. 2020;14(4):4096-4110. doi:10.1021/acsnano.9b08818
46. Serra A, Del Giudice G, Kinaret PAS, et al. Characterization of ENM dynamic dose-dependent MOA in lung with respect to immune cells infiltration. *Nanomater (Basel, Switzerland)*. 2022;12(12):2031. doi:10.3390/nano12122031

47. Jackson P, Halappanavar S, Hougaard KS, et al. Maternal inhalation of surface-coated nanosized titanium dioxide (UV-titan) in C57BL/6 mice: effects in prenatally exposed offspring on hepatic DNA damage and gene expression. *Nanotoxicology*. 2013;7(1):85-96. doi:10.3109/17435390.2011.633715
48. Bourdon JA, Halappanavar S, Saber AT, et al. Hepatic and pulmonary toxicogenomic profiles in mice intratracheally instilled with carbon black nanoparticles reveal pulmonary inflammation, acute phase response, and alterations in lipid homeostasis. *Toxicol Sci*. 2012;127(2):474-484. doi:10.1093/toxsci/kfs119
49. Bourdon JA, Williams A, Kuo B, et al. Gene expression profiling to identify potentially relevant disease outcomes and support human health risk assessment for carbon black nanoparticle exposure. *Toxicology*. 2013;303:83-93. doi:10.1016/j.tox.2012.10.014
50. Søs Poulsen S, Jacobsen NR, Labib S, et al. Transcriptomic analysis reveals novel mechanistic insight into murine biological responses to multi-walled carbon nanotubes in lungs and cultured lung epithelial cells. *PLoS ONE*. 2013;8(11):e80452. doi:10.1371/journal.pone.0080452
51. Solorio-Rodriguez SA, Williams A, Poulsen SS, et al. Single-walled vs. multi-walled carbon nanotubes: influence of physico-chemical properties on toxicogenomics responses in mouse lungs. *Nanomater (Basel, Switzerland)*. 2023;13(6):1059. doi:10.3390/nano13061059
52. Poulsen SS, Bengtson S, Williams A, et al. A transcriptomic overview of lung and liver changes one day after pulmonary exposure to graphene and graphene oxide. *Toxicol Appl Pharmacol*. 2021;410(November 2020):115343. doi:10.1016/j.taap.2020.115343
53. Bornholdt J, Saber AT, Lilje B, et al. Identification of gene transcription start sites and enhancers responding to pulmonary carbon nanotube exposure in vivo. *ACS Nano*. 2017;11(4):3597-3613. doi:10.1021/acsnano.6b07533
54. Nikota J, Williams A, Yauk CL, Wallin H, Vogel U, Halappanavar S. Meta-analysis of transcriptomic responses as a means to identify pulmonary disease outcomes for engineered nanomaterials. *Part Fibre Toxicol*. 2016;13(1):25. doi:10.1186/s12989-016-0137-5
55. Poulsen SS, Saber AT, Williams A, et al. MWCNTs of different physicochemical properties cause similar inflammatory responses, but differences in transcriptional and histological markers of fibrosis in mouse lungs. *Toxicol Appl Pharmacol*. 2015;284(1):16-32. doi:10.1016/j.taap.2014.12.011
56. Jackson P, Hougaard KS, Vogel U, et al. Exposure of pregnant mice to carbon black by intratracheal instillation: toxicogenomic effects in dams and offspring. *Mutat Res*. 2012;745(1-2):73-83. doi:10.1016/j.mrgentox.2011.09.018
57. Di Ianni E, Møller P, Cholakov T, Wolff H, Jacobsen NR, Vogel U. Assessment of primary and inflammation-driven genotoxicity of carbon black nanoparticles in vitro and in vivo. *Nanotoxicology*. 2022;16(4):526-546. doi:10.1080/17435390.2022.2106906
58. Danielsen PH, Bendtsen KM, Knudsen KB, Poulsen SS, Stoeger T, Vogel U. Nanomaterial- and shape-dependency of TLR2 and TLR4 mediated signaling following pulmonary exposure to carbonaceous nanomaterials in mice. *Part Fibre Toxicol*. 2021;18(1):1-18. doi:10.1186/s12989-021-00432-z
59. Oberdorster G. Significance of particle parameters in the evaluation of exposure-dose-response relationships of inhaled particles. *Inhal Toxicol*. 1996;8(8 Suppl):73-89. <http://www.ncbi.nlm.nih.gov/pubmed/11542496>
60. Schmid O, Stoeger T. Surface area is the biologically most effective dose metric for acute nanoparticle toxicity in the lung. *J Aerosol Sci*. 2016;99:133-143. doi:10.1016/j.jaerosci.2015.12.006
61. Jackson P, Hougaard KS, Boisen AMZ, et al. Pulmonary exposure to carbon black by inhalation or instillation in pregnant mice: effects on liver DNA strand breaks in dams and offspring. *Nanotoxicology*. 2012;6(5):486-500. doi:10.3109/17435390.2011.587902
62. Braakhuis HM, Park MVDZ, Gosens I, De Jong WH, Cassee FR. Physicochemical characteristics of nanomaterials that affect pulmonary inflammation. *Part Fibre Toxicol*. 2014;11(1):18. doi:10.1186/1743-8977-11-18
63. Oberdörster G, Oberdörster E, Oberdörster J. Nanotoxicology: an emerging discipline evolving from studies of ultrafine particles. *Environ Health Perspect*. 2005;113(7):823-839. doi:10.1289/ehp.7339
64. Vancza EM, Galdanes K, Gunnison A, Hatch G, Gordon T. Age, strain, and gender as factors for increased sensitivity of the mouse lung to inhaled ozone. *Toxicol Sci*. 2009;107(2):535-543. doi:10.1093/toxsci/kfn253
65. Vlahos R, Bozinovski S, Jones JE, et al. Differential protease, innate immunity, and NF- $\kappa$ B induction profiles during lung inflammation induced by subchronic cigarette smoke exposure in mice. *Am J Physiol Lung Cell Mol Physiol*. 2006;290(5):931-945. doi:10.1152/ajplung.00201.2005
66. Pottier N, Chupin C, Defamie V, et al. Relationships between early inflammatory response to bleomycin and sensitivity to lung fibrosis: a role for dipeptidyl-peptidase I and tissue inhibitor of metalloproteinase-3? *Am J Respir Crit Care Med*. 2007;176(11):1098-1107. doi:10.1164/rccm.200607-1051OC
67. Card JW, Carey MA, Bradbury JA, et al. Gender differences in murine airway responsiveness and lipopolysaccharide-induced inflammation. *J Immunol*. 2006;177(1):621-630. doi:10.4049/jimmunol.177.1.621
68. Mikkelsen L, Sheykhzade M, Jensen KA, et al. Modest effect on plaque progression and vasodilatory function in atherosclerosis-prone mice exposed to nanosized TiO<sub>2</sub>. *Part Fibre Toxicol*. 2011;8:1-17. doi:10.1186/1743-8977-8-32

## SUPPORTING INFORMATION

Additional supporting information can be found online in the Supporting Information section at the end of this article.

**How to cite this article:** Gutierrez CT, Loizides C, Hafez I, et al. Comparison of acute phase response in mice after inhalation and intratracheal instillation of molybdenum disulphide and tungsten particles. *Basic Clin Pharmacol Toxicol*. 2023;1-14. doi:10.1111/bcpt.13915